Accuracy Assessment of Stereo-Extracted Data From Airborne SAR Images♥

Thierry Toutin
Canada Centre for Remote Sensing
588 Booth Street
Ottawa, Ontario, K1A 0Y7

ABSTRACT

The paper presents a method and results of stereo extraction of planimetric and altimetric features from digital airborne SAR data on a low cost PC based stereo-workstation (DVP). A challenging study area was chosen in a mountainous area of Costa Rica. Accuracies of 24 m, 39 m and 40 m have been achieved for roads, creeks and DEM respectively. Better contrasts in the feature definition are a key point to improve planimetric positioning accuracies. If roads and creeks accuracies are almost independent of the location in the stereo-model, larger intersection angles enable a better DEM accuracy (around 20%). Surprisingly, the type of the relief does not affect the results, except for very shallow angles. The multiple stereo capability of RADARSAT will be a valuable source to ensure precise results of this research.

INTRODUCTION

The most recent development in photogrammetry is concerned with the move from an analytical to a digital ("softcopy") workstation . The main factors, which caused this fast development, can be summarised as follows:

- increasing availability of digital images;
- need for integration of raster and vector data;
- availability of powerful workstations; and
- low-cost, micro-computers compared to photogrammetric instruments...

This transition also applies to radargrammetry: one good example is the operational STARMAP system which was first developed on an analytical stereoplotter (Mercer et al., 1986) and further adapted to a digital stereo workstation (Leberl et al., 1991; Mercer and Griffiths, 1993). One interesting point which results from this transition is the combination of techniques and tools borrowed from photogrammetry and image processing, which somehow "blurred" the border between these two approaches.

As an example of such combined effects, topographic slope which frequently dominate over surface roughness and dielectric properties, accentuates even further the relief effect of a 3-D stereoscopic presentation. Inversely, two important elements in radar imaging

♥ Published in the International Journal of Remote Sensing, 1997, Vol. 18, No. 18, pp. 3693-3707.

STUDY SITE AND DATA SET

To look at the capabilities and the limits of the DVP system with radar data, a challenging area in the Cordillera Centrale in Costa Rica was selected. The study site is located in Provincia de Alajuela and overlaps two 1:50,000 scale maps: Aguas Zarcas and Quesada. This area is characterised by high relief where the elevation ranges from 200 metres along Rio Platanar to 2000 metres on Cerro Platanar. It is a rugged topography of young volcanic terrain highly dissected by a humid tropical climate, generating steep cliffs and deep gorges (20 to 100 metres) for the creekbeds.

The imagery consists of two airborne SAR images acquired in nadir mode by the SAR sensor of CCRS during the SAREX-92 mission in Central and South America (Elizondo et al., 1993). Both images, C-HH, are in slant range presentation (4.0 m in range by 4.31 m in azimuth). The nadir mode offers the greatest challenge because the viewing angles range from 0° at near edge of the swath to about 84° at the far edge. According to the standard terminology in photogrammetry, the viewing angle θ is the angle at the sensor between the range vector and the nadir vector. Near vertical viewing leads to large distortion in radar imagery, and large variations between the two images at the steepest viewing angles (0° - 40°).

The stereo coverage is formed with two images viewing the terrain from the same side. As shown in Figure 1, the angle between the two range vectors, the intersection angle Δθ, varies over a large range over the portion of the overlapping imagery. The intersection angle varies from approximately 55° at near range of the stereo-model to approximately 12° at far range of the stereo-model and this leads to large distortion variation for the parameters of the stereo model (Toutin, 1995a). Unfortunately, differential Global Positioning System (GPS) was not available for track recovery, and there are uncertainties in the flight line separation and aircraft altitude. Also, Figure 1 is illustrative in the sense that the terrain is not flat, compounding the uncertainty in the viewing and intersection angles.

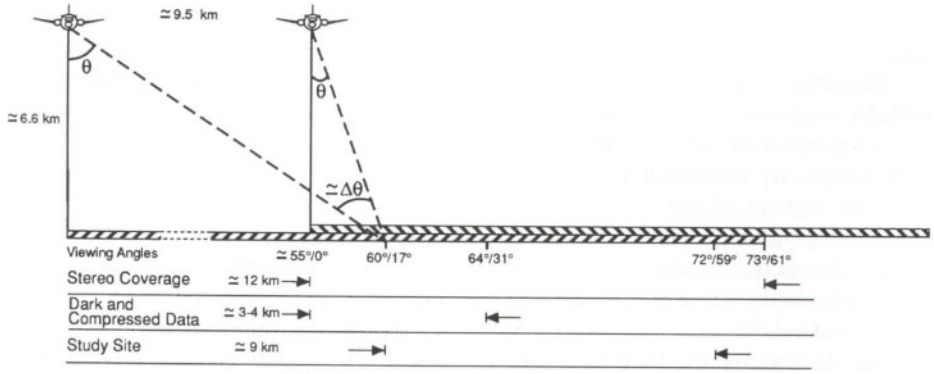

Figure 1: Radar (CCRS nadir mode) stereo-coverage on the study (θ: viewing angles; Δθ: intersection angle). Distances and angles are approximate due to the uncertainties in aircraft altitude and position, the relief and in the precise position of the nadir return.

benefit from stereoscopic viewing of an overlapping pair: it enhances interpretability due to three-dimensional viewing (Koopmans, 1974), and it permits correction of image geometry and separation of those backscatter effects due to slope (Guindon et al., 1990).

Stereoscopic viewing also permits the 3-D measurement of ground co-ordinates from images through mathematical reconstruction of the 3-D terrain model. Since Rosenfield (1968), numerous authors have formulated rigorous side-looking radar projection equations, similar to photogrammetric equations. Some of these equations have been adapted to process stereo radar data, and have been implemented on digital stereo workstations (Leberl et al, 1991; Geospace and Joanneum Research , 1992; Mercer and Griffiths, 1993; Toutin, 1995a).

In some of these stereo-workstations data has to be resampled to a "common quasi-epipolar geometry" in which the stereo-view and measurements are applied. However, resampling degrades the image geometric and radiometric quality (Gugan and Dowman, 1986) and will likely affect the qualitative interpretation and quantitative information extraction. Furthermore, the different results do not show the stereo restitution accuracy of conventional planimetric features such as roads, creeks, forest, etc. consistent with a 1: 50 000 map standard. Radar image content and interpretation have to be taken into account in the final accuracy of the feature extraction.

Accuracy is also a function of the stereo configuration. Domik (1984) shows with different test observers that the "best" subjective stereo impressions were obtained from simulated images when look angles were 50° and 70°, with a stereo intersection angle of 20°. The "realism" of the simulation can affect the validity of the conclusions because Kaupp et al. (1983) found that optimum stereo angles are at 40° - 45°.

Furthermore, stereo viewability and stereoplotting are different concepts because the lack of lower spatial frequency in the radiometry makes stereo viewing very difficult, and the lack of higher frequency does not make precise pointing possible (Fullerton et al., 1986). Consequently good stereo viewability does not induce necessarily an accurate stereo plotting, and vice versa.

The viewability of stereo radar has always been a great element of uncertainty in all stereo-radargrammetric work. Viewability effects on accuracy were addressed with multiple incidence angle SIR-B experiments (Leberl et al., 1986). It showed the best stereo viewing and plotting when the intersection angle was small (5° vs 23°), inversely to the radar-grammetric accuracy predictions. The extent of this difference and of the compromise between a good-vertical exaggeration and a good similarity between the image is not well understood yet.

In preparation for multi-mode and incidence angle data from RADARSAT, it is important to address more quantitatively some geometric and radiometric effects of influencing factors on stereo viewing and measurement accuracy. An experiment with stereo airborne radar over a high relief terrain in Costa Rica was then performed using a digital stereo workstation, the DVP. The accuracy of feature extraction in planimetry and

altimetry are evaluated as a function of different geometric and radiometric parameters related to the sensor, the stereo geometry and the terrain.

As the first results of this experiment have already been presented (Toutin, 1995a), this paper summarises the main characteristics of the DVP system, describes the data set, and presents the accuracy evaluation of the stereo extraction of planimetric features (roads, creeks), and altimetric features (spot height, digital elevation model, DEM), when compared to check stereo-compiled data from aerial photographs.

DVP SYSTEM

The stereo workstation DVP was originally designed at the "Département de photogrammétrie de l'Université Laval (Québec, Canada)" as a teaching and training tool for students in photogrammetry. It evolved as a low-cost general purpose digital stereo workstation to process aerial and terrestrial photos using standard photogrammetric solutions (Gagnon et al., 1990). Subsequently, the system has been adapted to visible and infra-red (VIR) satellite data, as well as airborne and satellite SAR images (Toutin, 1995a, 1995b) at the Canada Centre for Remote Sensing (CCRS).

The software is designed to run on a standard personal computer (PC) equipped with an inexpensive graphic card, and a digitising tablet. The stereo viewing is related to conventional photogrammetric viewing with the split screen method and a simple stereoscope. By preferring to move the measuring marks across stationary image windows instead of panning the images, low cost graphic card replaces the very expensive graphic processors required in many other digital stereo workstations.

The geometric modelling uses the collinearity and co-planarity conditions as in photogrammetry benefiting also from theoretical work in celestial mechanics (Toutin, 1983), and relates the Cartesian map co-ordinates to the radar co-ordinates (time or line, slant range distance or pixel). Further details on the geometric modelling and its applicability to visible and radar images can be found in Toutin (1995c). The formulation and its inversion are straightforward and thus one does not need to resample the images in a "common quasi-epipolar geometry", and the real time loop does not need a powerful real time processor, which has facilitated the implementation method on a low-cost PC.

The control of image positioning then follows the dynamic change to cancel the Y-parallax from the raw imagery, and retains real time performance in the stereo viewing and plotting. When the operator cancels the X-parallax to fuse the two floating marks of the measured point, a 3-D stereo-intersection is performed. Cartographic co-ordinates (planimetry and height) in the user defined map projection system are determined in real time for the measured point using a least square intersection process based on the equations and parameters of the geometric modelling.

Figures 2 and 3 show examples of these distortion variations between the two images at the near edge ($\Delta\theta \approx 40°$) and the far edge ($\Delta\theta \approx 10°$) of the stereo pair, respectively. Figure 2 (near Florencia City: 200-m elevation) shows large distortions between the two sub-images (506 x 600 pixels) due to the compression of planimetric scale from far to near range. Therefore, the stereo viewing is limited locally around the floating marks, but the stereo plotting on specific targets (road, field, forest) is possible. The right image includes a dark region, which corresponds to receiver noise prior to the first radar returns from the terrain below the aircraft (the so-called nadir return). Immediately after the nadir returns (to the right) the image is very compressed, the incidence angle changes very rapidly, and data interpretation is very difficult until an incidence angle of approximately 20° to 30° is reached. Consequently, approximately the first 3-4 km (in ground range) for the right image is not used in the analysis, and the ground range overlap region for the stereo restitution and accuracy evaluation is approximately 9 km (Figure 1).

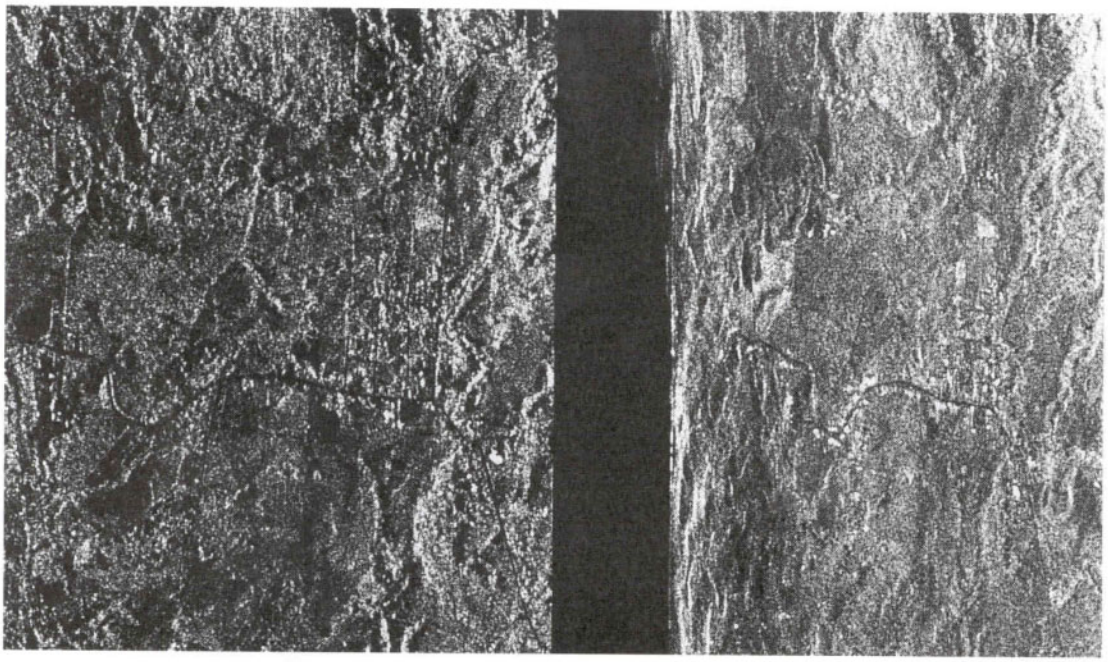

Figure 2: Stereo-sub-images (506 x 600 pixels) at the near edge of the stereo-model Florencia City: 200-m elevation).

Figure 3 (near Cerro Platanar: 2 183-m elevation) shows almost no distortion variation between the two sub-images (506 x 600 pixels), but the effect of shadowing along the lava flow and in the backslope of the volcano makes the precise stereo-plotting difficult even if stereo-viewing is possible.

The ground control points (GCP's) were obtained from the Instituto Geografico Nacionale (IGN) of Costa Rica and was stereo compiled from 1:60,000-scale aerial photographs taken in 1982, with an accuracy of five metres in X, Y and Z. This accuracy is sufficient compared to results (15-25 m) obtained with this geometric modelling from previous experiments (Toutin et al., 1992). The planimetric features (roads, creeks, forests) and the hypsography with a contour interval of 20 m were stereo compiled by the Canada

Centre for Mapping (Ottawa, Canada) using the same photographs. They were observed on the surface of the Earth in X, Y and Z UTM co-ordinates without movement of the feature due to a cartographic generalisation. The planimetric positioning accuracy is 5 m and the altimetric accuracy is 10 m.

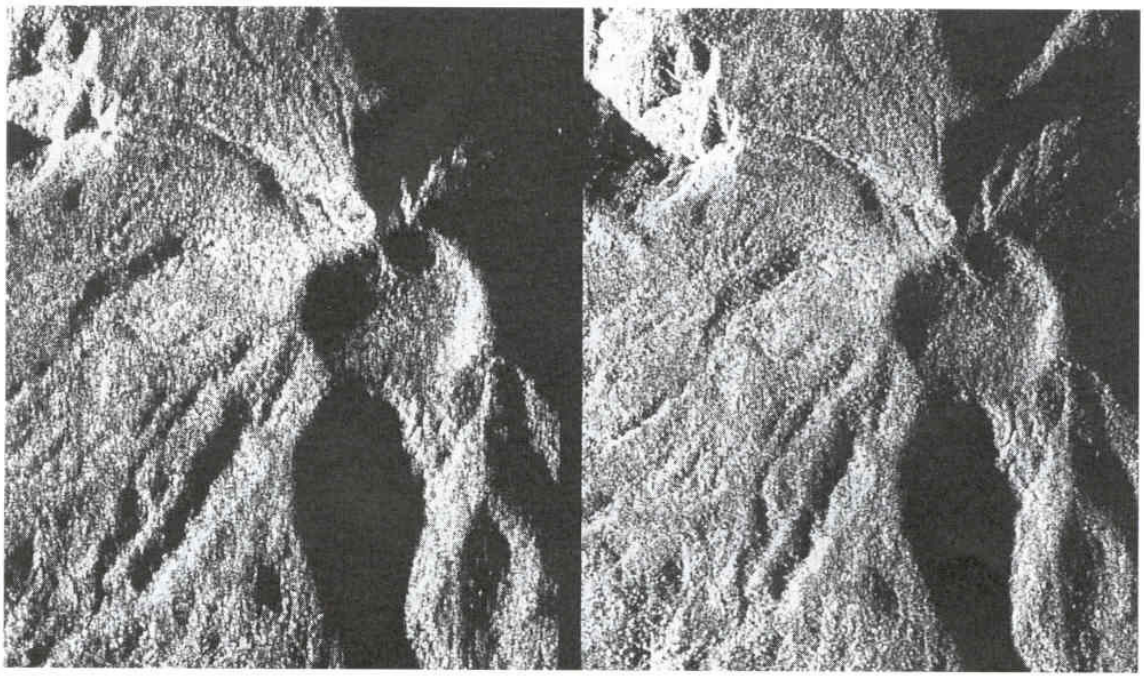

Figure 3: Stereo-sub-images (506 x 600 pixels) at the far edge of the stereo-model (Cerro Platanar: 2 183-m elevation).

EXPERIMENT

The different processing steps, the algorithmic aspects and the first results for this experiment have been explained by Toutin (1995a). To summarise, the digital data are first transferred to the DVP: it includes the SAR images, the SAR parameters (viewing angle, direction, resolution), the flight parameters (velocity, altitude, track) and the Earth surface parameters (semi-major axis, eccentricity). The geometric modelling parameters are first computed from these parameters, and further refined using the GCPs co-ordinates with an iterative least square bundle adjustment. The a-priori stereo mapping accuracy assessment is given with GCPs residuals in the order of 15 m, 20 m and 30 m for X, Y, Z, respectively. Errors on 50 independent check points were 17 m, 36 m and 48 m for X, Y, Z, respectively. More details of the accuracy assessment can be found in Toutin (1995a).

In the next step, the data (roads, creeks, forest boundaries and DEM) are then stereo-extracted visually in the radar stereo-model by an operator, transferred to ARC/INFO using a bi-directional translator developed by ESRI Canada in Montréal, cleaned and

edited using different GIS functions of ARC/INFO. In the same way, a translator was used to import the checked topographic data into the ARC/INFO environment.

For each extracted planimetric feature, a first qualitative comparison was made between the topographic file and the DVP file to look at the omission and commission errors. In a second step, buffered zones centred on the topographic features were generated at 5, 10, 13, 16, 19, 22, 25, 30 and 40 m for the roads, and at 10, 20, 30, 35, 40, 45, 50 and 60 m for the creeks and forest boundaries. They are used to quantify the cumulative linear distance of stereo-extracted DVP features within each zone. The percentage and the cumulative percentage of linear distance can then be computed for each zone.

The variation in the buffered zones for roads and creeks is mainly due to a better positioning accuracy expected for the roads than for the creek or the forest, in which radar image content, feature definition and interpretation have to be considered and play a role in the final accuracy. Figure 4 shows an example of the buffered zones, centred on the roads of the topographic file. The black line corresponds to the DVP feature to be compared.

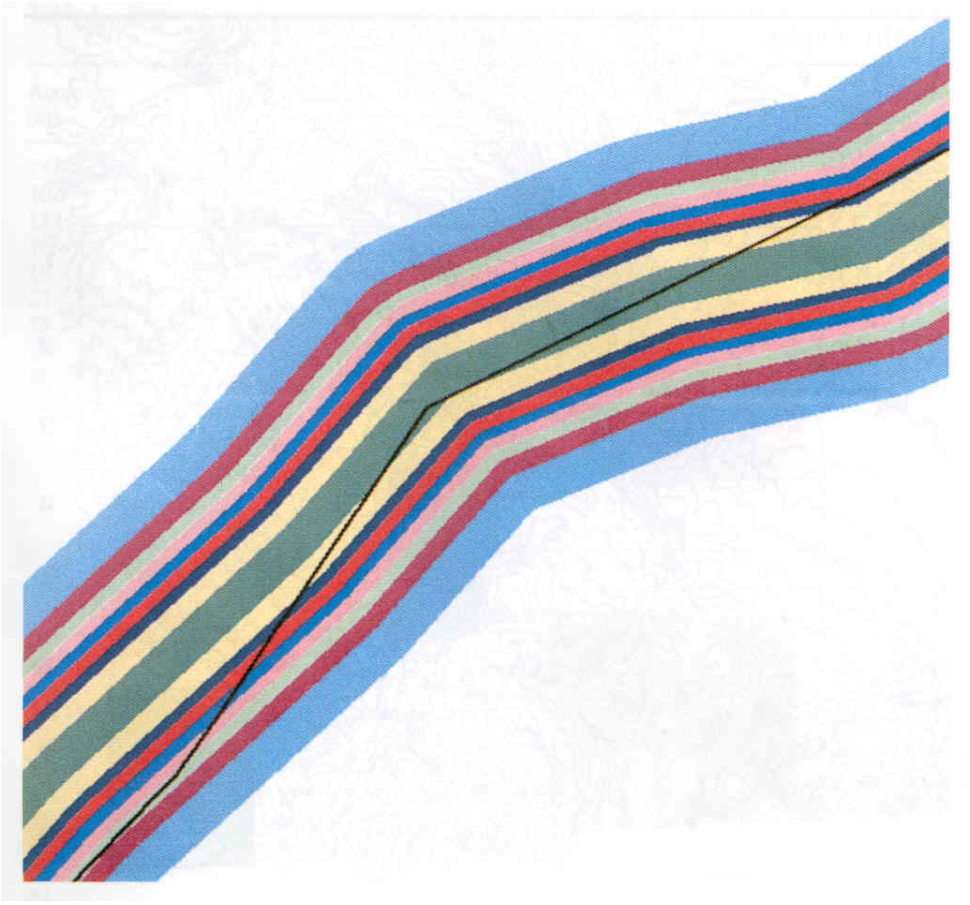

Figure 4: Buffered zones centred on the roads of the topographic file. The black line is the stereo extracted road from the airborne SAR stereo pair.

For altimetric features, 7100 points have been extracted to create five irregular small DEM (1 x 1 km, ..., 3 x 3 km) spread over the stereo pair in different image and terrain locations (Figure 5) to quantify the accuracy as a function of different parameters (viewing and intersection angles; flat to rugged terrain; forest or field area, etc.). These points are directly compared to the DEM generated with a fine grid spacing from the contour lines. This avoids errors generated by any processing to transform these irregular DEM's into a regular grid.

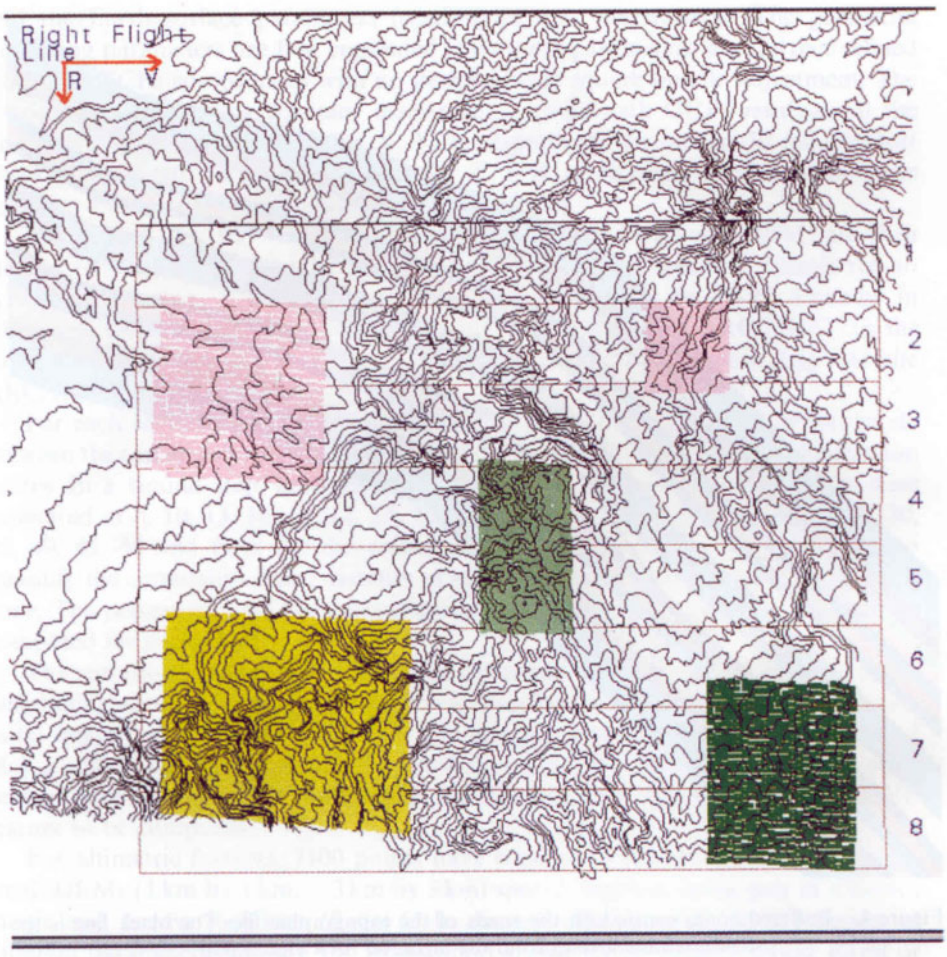

Figure 5: Location of the 5 DEM and the 8 strips over the topographic contour lines in the stereo-model. The red arrows are the azimuth (V) and illumination (R).

ACCURACY ASSESSMENT

Commission and omission errors

For the roads, there was no commission error, and the omission error, less than 2%, resulted from roads located at the near edge of the stereo-model where range compression

occurred for the right image. Some of this 2% omission error was also loose surface or gravel roads located in the mountainous area.

For the creeks, the commission error (less than 5%) and the omission error (around 10%) resulted from the physical characteristics of the creeks in this type of relief and in this tropical climate: they are small in width, engulfed in deep gorges, dry most of the time, and their source is almost impossible to locate.

For the forest boundaries, the commission error (less than 5%) and the omission error (about 30%) resulted from the definition of forest in topographic mapping. Furthermore, the operator is not a specialist in radar backscatter analysis nor in forestry applications. Consequently, the interpretation of image content biased the accuracy assessment for this specific feature, and this feature will not be used in future evaluations.

Positioning Accuracy Assessment for Roads

Table 1 gives the general results for the roads. For each buffered zone the linear distance inside the zone is computed using the ARC/INFO function; this enabled the percentage and the cumulative percentage to be computed for each zone. It shows a 24-m root mean square (RMS) accuracy (66%), and that there is no bias (larger than 5m) because the percentage decreases proportionately to the size of the zone until the 30m zone. After the 30 m zone, one can note larger percentages: 24.5% have errors greater than 30m. Each linear entity that had an error greater than 30 m was visually compared by importing the map file into the DVP. The origins of most of these errors were due to misinterpretation related to radiometric problems (poor contrast, roads lost within the context), or to effects specific to radar (slant range compression, shadow in the backslope, foreshortening). It was also visually checked there is no error larger than the tolerance (±3 times RMS error).

Table 1: General Results of the Comparison for Roads between the Checked Data and the DVP Extracted Data.

Accuracy (metres)	**Distance (metres)**	**Percentage (%)**	**Cumulative percentage**
5	13,065	19.8	12.8
10	10,131	15.4	35.2
13	5,799	8.8	44.0
16	4,614	7.0	51.0
19	4,041	6.1	57.1
22	3,846	5.8	62.9
25	3,262	4.9	67.8
30	4,997	7.6	75.4
40	7,369	11.2	86.6
40+	8,864	13.4	100
Total	65,987	100	

Table 2 gives only the cumulative percentage results as a function of different parameters: parallel or perpendicular to the radar illumination, "in" and "out of the cities". Roads perpendicular to radar illumination to flight lines have a RMS accuracy of 19 m versus 27 m for roads parallel to radar illumination. Ditches and trees along the roads act as a dihedral corner reflector. Therefore, the sides of roads perpendicular to radar illumination define better the roads from the surroundings when surface roughness is the same.

Table 2: Roads Results as a Function of Geometric or Radiometric Parameters

Accuracy (metres)	Cumulative percentage			
	Perpendicular to range direction	Parallel to range direction	In the cities	Out of the cities
5	20.6	19.1	30.4	14.8
10	41.2	31.1	49.5	28.4
13	52.3	38.4	59.9	36.4
16	60.3	44.7	68.3	42.7
19	66.1	51.1	73.9	49.1
22	71.7	57.1	80.5	54.6
25	75.9	62.5	85.1	59.7
30	81.5	71.4	90.3	68.4
40	88.4	85.3	98.6	80.9
40+	100	100.0	100.0	100.0

Roads "in the cities" have a RMS accuracy of 15 m versus 28 m for roads "out of the cities". Furthermore, larger errors (over 40 m) occur for the roads "out of cities". The two main reasons are: the city building acts as dihedral corner reflector which define very well the roads, and mis-interpretations occur for roads "out of the cities" due to less contrast in the backscatter.

Figure 6 is the last accuracy assessment as a function of the stereo-geometry, i.e. the viewing angles and the intersection angle. The stereo model was cut out in nine 1-km wide strips parallel to the flight lines (Figure 5). The intersection angle is computed at the middle of the strip, and each strip corresponds to a few degrees variation for the intersection angle. On the last strip, there were not enough data (few hundred metres) to give a valid evaluation of the accuracy. When the intersection angles (on the X-axis of Graph 1) decreases from left to right, the stereo geometry becomes weaker, and the stereo viewing becomes better. The three better accuracies (less than or equal to 18 m) is due to 40 to 50% of the roads in these three strips which are "in the cities", then with a better accuracy as mentioned before. For the two extreme strips, the worse accuracies can be accounted for:

- the different characteristics specific to the radar (planimetric scale compression at the near edge, and shadowing at the far edge) as explained above and illustrated in Figures 2 and 3; and

- the amount of roads extracted in both strips are smaller (3 km versus 10 km) compared to the other strips.

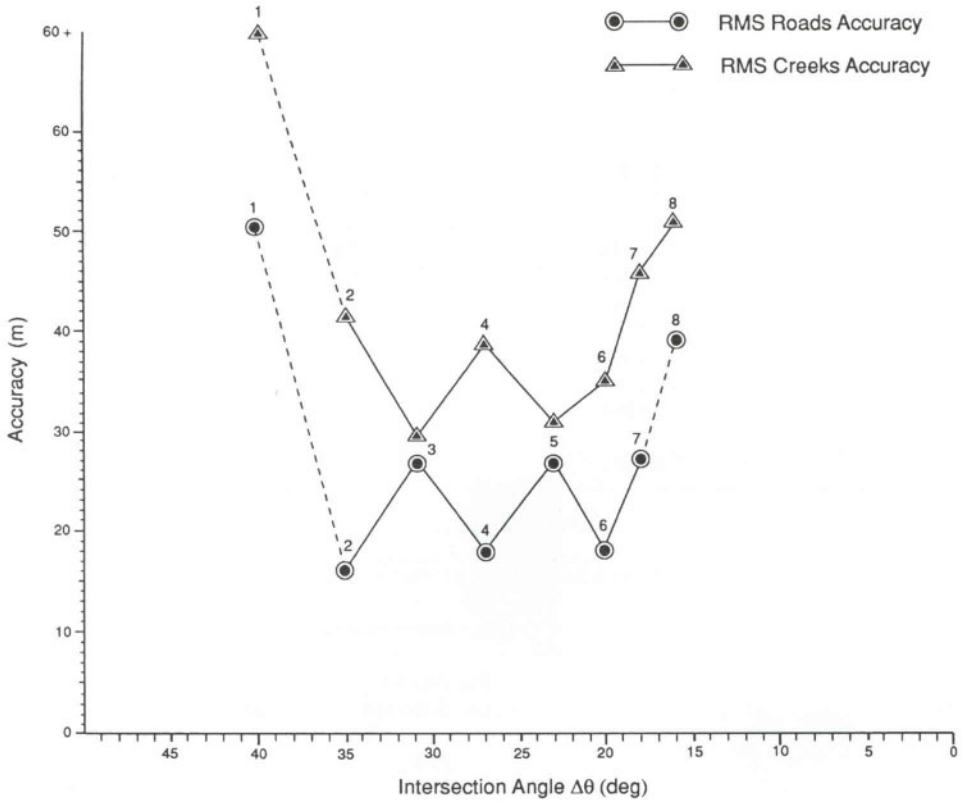

Figure 6: RMS accuracies (metres) for roads and creeks as a function of the intersection angle (numbers are related to the eight strips).

Positioning Accuracy Assessment for Creeks

Therefore, the reliable ranges for intersection angle to achieve the 20m accuracy between 35° and 18°, for which no correlation with accuracy has been found. Table 3 and Figure 6 give the results for the creeks all together and as a function of the intersection angle, respectively. A 39 m RMS accuracy with no bias larger than 10 m is achieved (Table 3), but with some large errors over 60 m. Similarly as for the roads, Graph 1 does not show any correlation between accuracy and intersection angle. For the first strip (40°-intersection angle), only 900 m of creeks (compared to 7-11 km for the others) were used to compute the statistics, which does not give enough confidence for this strip.

These worst results for creeks compared to the roads resulted from the particular physical characteristics of the creeks and from this particular study site: a volcanic and tropical area. Most of the time, the creek beds are too small and hidden in the deep gorges. Therefore, they are extracted by following thalwegs as is done with aerial photographs. For this feature, the accuracy described in Table 3, then, combines planimetric, altimetric, image content, and interpretation errors, in which the last three play a larger role than

they do for the roads. Thus these results for the creeks do not reflect the general restitution accuracy of the airborne SAR data with the DVP system, but are specific to this type of topographic feature: intermittent watercourse.

Table 3: General Results of the Comparison for Creeks between the Checked Data and the DVP Extracted Data

Accuracy (metres)	**Distance (metres)**	**Percentage (%)**	**Cumulative percentage**
10	16 403	21.7	21.7
20	14 323	19.0	40.7
30	11 661	15.5	56.2
35	4 304	5.7	61.9
40	3 715	4.9	66.8
45	3 978	5.3	72.1
50	3 255	4.3	76.4
60	4 502	6.0	82.4
60+	13 291	17.6	100.0
Total	75 432	100.0	

Elevation Accuracy Assessment

For the height measurements, a first evaluation was performed to quantify the altimetric pointing accuracy. Eleven points on each strip, which span different features and cover type such as wood, rock or clearcut area, roads, cliffs, etc., were chosen. It should be noted that these are not necessarily identifiable features. By pointing on all of these features in each strip two times (about 200 pointings), one gets estimation for the altimetric pointing accuracy of ±7.1 m. Furthermore, there is no significant difference (around 1 m) between the different strip results. The same test was done for high, middle and low reliefs and gave similar results (±6.9 m), without significant variations between the different reliefs.

The second evaluation is done by comparing the 5 irregular DEM's to the topographic DEM. The statistics generated from all 7100 points together give:

- RMS error: ±39.6 m Error min.: -85.0 m
- Bias: +29.0m Error max.: +125.0 m

Compared to the absolute altimetric errors (30.3 m for well-identifiable points and 38 m for other points) presented in the first results (Toutin, 1995a), the 39.6 m RMS error for the DEMs is consistent. Furthermore there is no blunder out of tolerance (bias ±3 RMS error).

The bias comes from the operator who plots always at lowest altitude. It has been checked with other data (aerial photo, SPOT panchromatic, ERS-1 SAR) on other study

sites (Toutin, 1995b). This bias is specific for each operator in the stereo-plotting, and can be computed and corrected for each type of data.

Figure 7 gives another evaluation of the DEM accuracy (bias and RMS error) as a function of the intersection angle. For the first strip, the results are not significant because statistics have been generated with only 25 points. For the other strips, one can note:

- a small correlation between the RMS error and the intersection angle. The RMS errors are smaller at the near half edge of the stereo model where the intersection angle is larger; and
- a trend for the bias going from negative to positive values as the intersection angle decreases. That corresponds likely to a "bad levelling" of the full stereo model in the range direction. For the larger bias errors (-38m and +60m), at that time there is no explanation, mainly when compared to smaller bias errors for the adjacent strips.

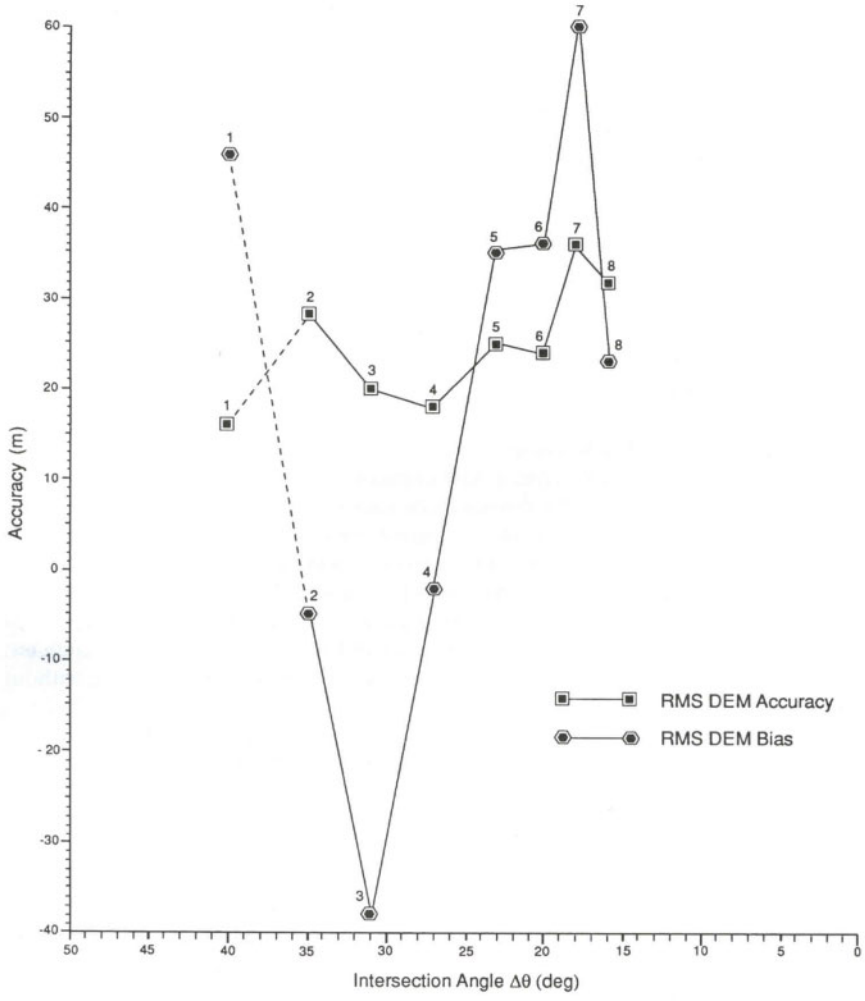

Figure 7: RMS accuracy and bias (metres) for DEM as a function of the intersection angle (numbers are related to the eight strips).

This trend can be accounted for, partly because the terrain elevation variation (about 1000 m over 9 km) occurred mainly in the range direction, and partly because the variation of the intersection angle for the CCRS nadir mode leads to larger errors than other CCRS modes or airborne SAR systems (Toutin, 1995a). But, these bias are also combined with the previously mentioned operator bias because the positive values of the bias are larger than the negative values. This "bad levelling" could easily be corrected in post-processing, with some known elevation points spread in the range direction.

The last evaluation for the DEMs is to combine DEM points in low, medium and high relief categories. Statistics give:

- for low relief with 1100 points:

RMS error:	±31.2 m	Error min.:	- 85.0 m
Bias:	-16.1 m	Error max.:	+ 77.0 m

- for medium relief with 1700 points:

RMS error:	±30.2 m	Error min.:	- 75.0 m
Bias:	+20.5m	Error max.:	+ 93.1 m

- for high relief with 4300 points:

RMS error:	±38.0 m	Error min.:	- 49.3 m
Bias:	+48.2 m	Error max.:	+ 125.0 m

There is a small improvement in the low and medium reliefs. Some larger errors in the high relief can be imputed to shadowing effect as mentioned earlier (Figure 3), mainly because the high relief terrain is located at the far edge of the stereo model with viewing angles of 60° - 70°. Less radar shadow with steeper angles should improve the DEM accuracy in high relief terrain to about the same accuracy level as the medium relief terrain. The different bias are also consistent with the previous results (bad levelling), because the low relief terrain is located at the near edge of the stereo model, the medium relief terrain at the middle and far edge, and the high relief at the far edge.

CONCLUSIONS

This paper has presented accuracy evaluation of feature extraction from digital airborne stereo SAR data using a photogrammetric approach on a PC based stereo workstation. The stereo extracted features have then been compared in a GIS environment, to checked topographic features from 1:60 000 stereo compiled aerial photographs (planimetric positioning accuracy of 5m and altimetric accuracy of 10m). Planimetric and altimetric accuracies have been computed for roads, creeks, forest boundaries and for irregular DEM. Evaluation of these accuracies has also been done as a function of different geometric and radiometric parameters (feature definition, orientation, location, contrast, relief, etc.).

In planimetry, the general accuracies for roads and creeks are 24m and 39m, respectively, without error out of tolerance. This difference comes mainly from the physical characteristics of each feature and their definition in the radar image. For the forest boundaries, too many variations due to its topographic definition, the image content and interpretation are noted to give a valuable accuracy assessment. Roads perpendicular to the range direction or "in the cities" are 30% to 45% more accurate than roads parallel to the range direction or "out of the cities", respectively. Differences result from a better contrast of the road sides (ditches, trees, buildings) which act as a dihedral corner reflectors. Finally, roads and creeks accuracies are almost independent of the location in the stereo-model, i.e. of the intersection angles along the range direction.

In altimetry, a general accuracy of 39.6 m with a 29 m bias have been computed for the DEM extraction without error out of tolerance. The bias is due to an operator who systematically stereo plotted at lower altitude. This phenomenon is well known in stereo photogrammetry with aerial photographs, it seems to be confirmed with remote sensing data. The type of relief (low, medium, or high) does not affect this accuracy, but the location in the stereo model does: steepest angles produce larger intersection angles which enable a better accuracy, around 20%, to be achieved. A differential bias has been noted resulting from a "bad levelling" in the range direction; but this bias could be corrected with some known elevation points.

The multiple stereo-capabilities of RADARSAT with its different viewing angles will be a valuable data source for stereo SAR processing slides to precise the results of this research. It will then provide more possibilities to evaluate different stereo configurations for the same test site to better evaluate the accuracy of planimetric and altimetric features in different terrain configuration as a function of different radiometric and geometric parameters. Future studies should give us a better understanding of the factors influencing stereo radar accuracies, because in general, reported results from the literature seems so far incoherent (Leberl, 1990).

ACKNOWLEDGEMENTS

The author would like to thank IGN Costa Rica and Mr. Carlos Elizondo for the data and useful information necessary to complete this project. He would like to thank his CCM and CCRS colleagues, particularly Dr. Brian Brisco and Dr. Réjean Simard for their critical review to improve this paper. He also thanks Ms. Liyuan Wu and France Tessier of Consultants TGIS Inc., for the data processing and software adaptation.

REFERENCES

Domik, G., 1984. Evaluation of Radar Stereo Viewability by Means of Simulation Technique, *Proceedings IGARSS '84*, Paris, France, ESA-SP-215, (Paris: ESA), pp. 643-646.

Elizondo, C.L., N. Beaulieu, R.K. Raney, F. Ahern and Fr. Campbell, 1993. Proyecto Radar/Costa Rica: A Collaborative Research Project, *Proceedings of the 16th Canadian Symposium on Remote Sensing*, Sherbrooke, Quebec, (Ste Foy: Association québécoise de télédétection), pp 61-65.

Fullerton, J.K., F. Leberl and R.E. Marque, 1986. Opposite Side SAR Image Processing for Stereo Viewing, *Photogrammetric Engineering and Remote Sensing*, 52(9):1487-1498.

Gagnon, P.A., J.P. Agnard, C. Nolette and M. Boulianne, 1990. A Microcomputer-based General Photogrammetric System, *Photogrammetric Engineering and Remote Sensing*, 56(5):623-625.

Geospace and Joanneum Research, 1992. Remote Sensing Software Package Graz - Software for Geometric Treatment of Multisensor Remote Sensing Data, *Colour Brochure*, DIBAG, Graz, Austria, 10 pages.

Gugan, D.J. and I.J. Dowman, 1986. Design and Implementation of a Digital Photogrammetric System, *Proceedings of Commission 2 ISPRS Symposium*, Baltimore, MD, (Falls Church: ASPRS), pp. 100-109.

Guindon, B., J.W.E. Harris, P.M. Teillet, D.G. Goodenough, J.F. Meunier, 1980. Integration of MSS and SAR Data for Forested Region in Mountainous Terrain, *Proceedings of the 14th International Symposium of Remote Sensing for Environment*, San Jose, Costa Rica, (Ann Arbor: ERIM), pp. 1673-1690.

Kaupp, V., L. Bridges, M. Pisaruk, H. MacDonald and W. Waite, 1983. Simulation of Spaceborne Stereo Radar Imagery - Experimental Results, *IEEE Transactions on Geoscience and Remote Sensing*, GE-21(3): 400-405.

Koopmans, B., 1974. Should Stereo SAR Imagery be Preferred to Single Strip Imagery for Thematic Mapping? *ITC Journal*, 1974-3, Enschede, The Netherlands, pp. 424-444.

Leberl, F., G. Domik, J. Raggam and M. Kobrick, 1986. Radar Stereomapping Techniques and Application to SIR-B Images of Mt Shasta, *IEEE Transactions on Geoscience and Remote Sensing*, GE-24(4): 473-480.

Leberl, F., 1990. Radargrammetric Image Processing, *Artech House*, Norwood, MA, U.S.A.

Leberl, F.W., M. Millot, R.S. Wilson, M. Karspeck, B. Mercer, and S. Thornton, 1991. Radargrammetric Image Processing with a Softcopy Stereo Workstation, *Proceedings of the Eighth Thematic Conference on Geologic Remote Sensing*, Denver, CO, U.S.A. (Ann Arbor: ERIM), pp. 639-647.

Mercer, J.B., R.T. Lowry, F. Leberl and G. Domik, 1986. Digital Terrain Mapping with STAR-1 SAR Data, *Proceedings of the IGARSS '86 Symposium*, Zurich, Switzerland, (Paris: ESA), pp. 645-650.

Mercer, B. and S.C. Griffiths, 1993. Operational Topographic Mapping from Airborne SAR Data, *Proceedings of the International Symposium on Operationalization of Remote Sensing*, Enschede, The Netherlands, (Enschede: ITC), Vol. 5: pp. 77-87.

Rosenfield, G.H., 1968. Stereo Radar Techniques, *Photogrammetric Engineering*, 34(6): 586-594.

Toutin, Th., 1983. Analyse mathématique des possibilités cartographiques du satellite SPOT, Mémoire du Diplôme d'Études Approfondies*, Ecole Nationale des Sciences Géodésiques*, Saint-Mandé, France, 74 pages.

Toutin, Th., Y. Carbonneau and L. Saint-Laurent, 1992. An Integrated Method to Rectify Airborne Radar Imagery Using DEM, *Photogrammetric Engineering and Remote Sensing*, 58(4): 417-422.

Toutin, Th., 1995a. Airborne SAR Stereo Restitution in a Mountainous Area of Costa Rica: First Results, *IEEE Transactions on Geoscience and Remote Sensing*, 33(2): 500-504.

Toutin, Th., 1995b. Generating DEM from Stereo-images with a Photogrammetric Approach: Examples with VIR and SAR Data*, EARSeL Journal "Advances in Remote Sensing"*, 4(2):110-117.

Toutin, Th., 1995c. Multi Source Data Integration with an Integrated and Unified Geometric Modelling, *EARSeL Journal "Advances in Remote Sensing"*, 4(2):118-129.